Octupolar perturbation of a single ion in a Penning trap

Martín Lara
Real Observatorio de la Armada, 11110 San Fernando, Spain

J. Pablo Salas
Area de Física Aplicada, Universidad de La Rioja, C/Madre de Dios 51, 26006 Logroño, Spain

(Received 13 June 2002; published 13 February 2003)

We investigate the classical dynamics of a single ion trapped in a Penning trap perturbed by a octupolar electrostatic perturbation that introduces nonlinearities in the motion. We show that the dynamics is controlled by a single external parameter that combines the influence of the electric and magnetic fields. Through the variation of this parameter, we explore the evolution of the phase space structure of the system by the numerical continuation of the families of periodic orbits.

DOI: 10.1103/PhysRevE.67.027401 PACS number(s): 52.25.Gj, 32.80.Pj, 39.10.+j, 05.45.−a

I. INTRODUCTION

The dynamics of a perturbed single ion Penning trap is investigated from the point of view of the classical mechanics. Classical dynamics has proven to be very useful for interpreting the quantum dynamics of atomic and molecular systems, even when the classical dynamics is chaotic and the quantum dynamics is strongly mixed [1]. The study of periodic orbits and phase space structure provides useful information that can be compared with the behavior of the corresponding quantum system and with experiments [1–3].

The Penning trap [4] provides three-dimensional trapping of charged particles by means of a magnetic field plus a quadrupolar electric field. The electric field is achieved by means of a set of three electrodes that are (ideally) infinite hyperboloids of revolution. However, when a real trap is considered, the electric field can be modeled by means of the multipole expansion [7]

$$V=\sum_{l\geqslant 0} V_l, \quad V_l=\sum_{0\leqslant k\leqslant l} a_{l,k} r^l \mathcal{P}_l^k(\cos\theta)\cos k\phi, \qquad (1)$$

where (r,θ,ϕ) are spherical coordinates, and $\mathcal{P}_l^k$ are the Legendre polynomials. The first two terms are linear, producing constant forces. The *quadrupole* V_2 gives rise to harmonic motion, and all higher orders introduce nonlinearities in the motion. In typical real Penning traps, the electrodes can be assumed to be symmetrical with respect the *x,y* plane and cylindrically symmetric. Hence, all the terms in Eq. (1) with l odd and $k\neq 0$ vanish. In this work, we consider the contribution of the *octupole* V_4 that is the main perturbation in a real trap where the electrodes are approximated by electrodes of spherical section [5]. Hence, by using cylindrical coordinates, we express the electrostatic potential $V=V_2+V_4$ as

$$V=U_0[2z^2-\rho^2+a(8z^4-24\rho^2z^2+3\rho^4)]/R_0^2, \qquad (2)$$

where $a=a_4/R_0^2$, U_0 is the voltage applied to the end-cap electrodes with respect to the ring, R_0 is the distance between the two end caps, and $\rho^2=x^2+y^2$.

The electric potential acts as a trap only along the z axis; while the magnetic field B along the z axis provides the complete trapping.

II. EQUATIONS OF MOTION

The Hamiltonian of a trapped single ion of mass m and charge q is

$$\mathcal{H}=\tfrac{1}{2}(P_\rho^2+P_z^2+P_\phi^2\rho^{-2})-(\tfrac{1}{2}qB)P_\phi+(\tfrac{1}{2}qB)^2\tfrac{1}{2}\rho^2 + mV(\rho,z), \qquad (3)$$

where (P_ρ,P_z,P_ϕ) are the conjugated momenta of the cylindrical coordinates (ρ,z,ϕ). Since the system is under rotation around the z axis, the canonical angular momentum P_ϕ is an integral. By introducing the ratio $\delta=w_z/w_c$ between the axial $w_z=\sqrt{4qU_0/(mR_0^2)}$ and cyclotron $w_c=qB/m$ frequencies, scaling time by w_c, and coordinates by R_0, we write Eq. (3) in dimensionless coordinates as

$$\mathcal{H}=\tfrac{1}{2}(P_\rho^2+P_z^2)+W(\rho,z;P_\phi), \qquad (4)$$

where W is the effective potential,

$$W=-\frac{P_\phi}{2}+\frac{P_\phi^2}{2\rho^2}+\frac{\rho^2}{8}+\frac{\delta^2}{4}[2z^2-\rho^2+a(8z^4-24\rho^2z^2 + 3\rho^4)]. \qquad (5)$$

As parameter a must be considered fixed for a given trap, the problem depends on the external parameter δ—giving a measure of the relative influence of the electric and magnetic fields—as well as on the internal one P_ϕ, and of course on the energy integral $\mathcal{H}=E$.

Because of the cylindrical symmetry of our problem, the (ρ,z) motion is decoupled from the angular motion, and the study of the equations of motion,

$$\dot\rho=P_\rho, \quad \dot P_\rho=-\partial W/\partial\rho, \quad \dot z=P_z, \quad \dot P_z=-\partial W/\partial z, \qquad (6)$$

of the (ρ,z,P_ρ,P_z) phase space will provide enough information on the behavior of the system. It is convenient to distinguish between the case $P_\phi\neq 0$, where a centrifugal bar-

rier exists preventing the orbits from approaching the origin, and the case $P_\phi=0$, where the motion takes place on a vertical plane that rotates with constant angular velocity. In this paper we focus on the case $P_\phi=0$, which is quite representative of the dynamics for all P_ϕ.

III. PHASE SPACE STRUCTURE

In the rotating (ξ,z) plane—where we use ξ instead of ρ in order to consider negative values—the potential energy surface $W(\xi,z)=E$ shows five critical points: a minimum P_0, and four symmetrically located saddle points $P_{1,2,3,4}$,

$$P_0=(0,0), \quad P_{1,2,3,4}=\frac{1}{2\delta}\left(\pm\sqrt{\frac{1+4\delta^2}{15a}},\pm\sqrt{\frac{1-\delta^2}{10a}}\right). \tag{7}$$

Hence, the effect of the octupolar perturbation is to create four equivalent channels of escape through which the ion is able to leave the trap. We remark that the saddle points are equilibria with respect to the rotating frame and circular trajectories with constant angular velocity in the inertial frame of the trap.

The energies of the critical points are

$$E_0=0, \quad E_S=E_{1,2,3,4}=\frac{1+8\delta^2-14\delta^4}{960\delta^2 a}. \tag{8}$$

When a increases, the energy E_S decreases, and the saddle points tend to the minimum. As expected, when the octupolar perturbation grows, the trapping energy interval and the zone where the ion can be trapped decrease. In addition, note that $E_S=E_0=0$ for

$$\delta_\ell^2=\frac{2+\sqrt{15/2}}{7}, \quad \delta_\ell\approx 0.823, \tag{9}$$

which does not depend on a. At this value the motion is not confined except for oscillations in the ξ and z directions—that are critical. Therefore we limit our study to values of δ in the interval $(0,\delta_\ell)$, where the ion can be trapped. Note that the possibility of escape is always present because in the interval $(0,\delta_\ell)$ there always exists a δ value for which the energy of saddle points can be smaller than the ion's energy.

The phase space structure is mainly characterized by the number of the periodic orbits living in phase space, and by their stability. The stability of a periodic orbit is determined from the eigenvalues λ_i of the monodromy matrix. In Hamiltonian problems, the eigenvalues appear in reciprocal pairs, and we have one trivial eigenvalue $\lambda_0=1$ with multiplicity 2. Then, the stability index

$$k=\lambda+1/\lambda \tag{10}$$

is normally used, where the condition k real and $|k|<2$ applies for linear stability, and the critical value $k=\pm 2$ means that a new family of periodic orbits has likely bifurcated from the original one.

Therefore, we proceed as follows. First, we identify the values of the parameters (P_ϕ,δ,a) for which periodic analytical solutions exist in the reduced phase space. Then, we carry out the numerical continuation of the families of periodic orbits—by varying one parameter, while the other remains constant—that arise from those solutions. In addition, a stability diagram presenting the evolution of k versus the parameter generator of the family is computed for every family, where we can detect possible bifurcations. When a bifurcation is found, the study is completed by calculating the corresponding Poincaré surfaces of section.

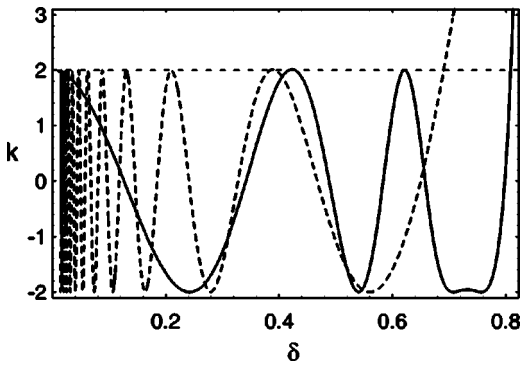

FIG. 1. Families of periodic oscillations on the z axis (dashed line) and on the ξ axis (full line).

In searching for particular solutions of Eq. (6), we find the following.

(1) Rectilinear orbits along the ξ axis $(z=0)$ that exist always, which we call R_ξ.

(2) Rectilinear orbits along the z axis $(\xi=0)$ that exist for $P_\phi=0$, which we call R_z.

(3) Rectilinear solutions with $z/\xi=\pm\sqrt{3/5}$ that exist for $P_\phi=0$ and $\delta=\sqrt{1/6}$.

(4) Circular solutions of radius $\xi^2+z^2=6E$ that exist for $P_\phi=0$, $\delta=\sqrt{1/6}$, and $a=0$.

Therefore, we have available four periodic solutions to start the continuation procedure. We first compute the family of quasi circular periodic orbits that emanate from the circular solution from variations of the structural parameter a until reaching the value $a=0.2$. For $a=0.2$ the electrodes are quite deformed and this value—that is near to experimental values [5]—will be considered fixed hereafter. Then, for $P_\phi=0$ we study the variation of all four solutions for variations of the control parameter δ.

In order to work in a regular region of confined motion but with possibility of escape, we fix the energy to $E=1/200$ for which value the escape channels are reached at

$$\delta^2=\frac{2}{7}-\frac{6a-\sqrt{3}\sqrt{125-80a+24a^2}}{35\sqrt{2}}, \tag{11}$$

which for $a=0.2$ gives $\delta\approx 0.786<\delta_\ell$, inside the working interval.

In Fig. 1 we see that oscillations on the ξ axis show a regular behavior with stable orbits $(|k|<2)$ for $\delta<0.809$ and possible bifurcations at $\delta\approx 0.242$, 0.423, 0.540, 0.623, 0.708, 0.756, 0.809. Oscillations on the z axis show stability for $\delta<0.6903$ and possible bifurcations at $\delta\approx 0.690$, 0.561, 0.390, 0.279, 0.210, 0.164, 0.131. For smaller values of δ the

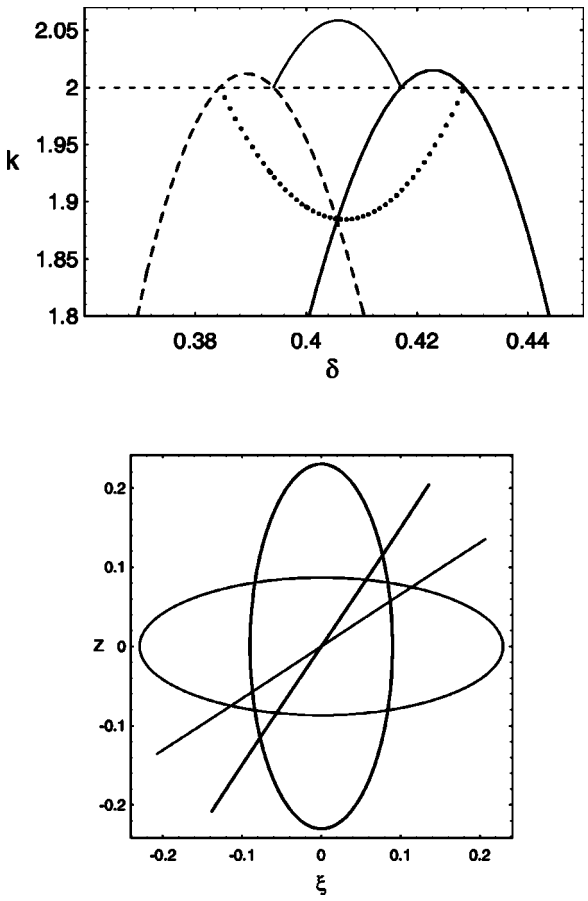

FIG. 2. Top: region of δ with stable, rectilinear, inclined orbits (dotted line), and unstable, elliptical ones. Bottom: orbits for $P_\phi = 0$, and $\delta = 0.397$ (black), $\delta = 0.414$ (gray).

stability behavior is highly oscillatory between the critical values ± 2 and, likely, with many bifurcations.

After a careful look at the values $\delta \approx 0.423$ and $\delta \approx 0.390$ given before, we see that not one, but two consecutive bifurcations are produced in their vicinity where the inclined, rectilinear orbits and the elliptic periodic solutions appear. As presented in Fig. 2, they only exist in a narrow interval of δ. Thus, the unstable, elliptic orbits bifurcate first from the z axis at $\delta \approx 0.385$ and immediately the stable, inclined rectilinear solutions bifurcate at $\delta \approx 0.394$. Both families terminate on the x-y plane: first the inclined, rectilinear trajectories at $\delta \approx 0.417$, and then the elliptic orbits at $\delta \approx 0.429$.

Figure 3 provides a representation of the reduced phase space for $P_\phi = 0$ and $\delta = 1/\sqrt{6}$, where we easily identify the stable rectilinear orbit along the ξ axis as the elliptic fixed point located at (0, 0); the rectilinear orbits $z = \pm\sqrt{3/5}\xi$ as the elliptic fixed points symmetrically located at the z axis; two unstable almost circular orbits traveled in opposite directions, as the hyperbolic fixed points of the separatrix that divides the previous regions of motion. Note that the stable oscillation on the z axis is not a tangent to the flux in this representation, and corresponds to the exterior limit of the Poincaré section $P_z = \sqrt{2E - \delta^2 z^2(1 + 4az^2)}$.

According to Figs. 1 and 2, a very different behavior is

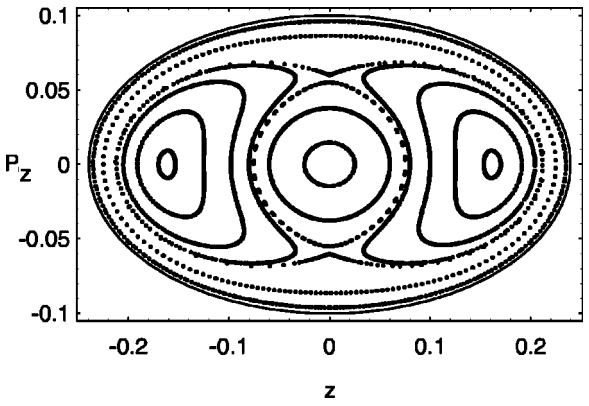

FIG. 3. Surface of section z-P_z ($P_\xi = 0$) for $\delta = 1/\sqrt{6}$.

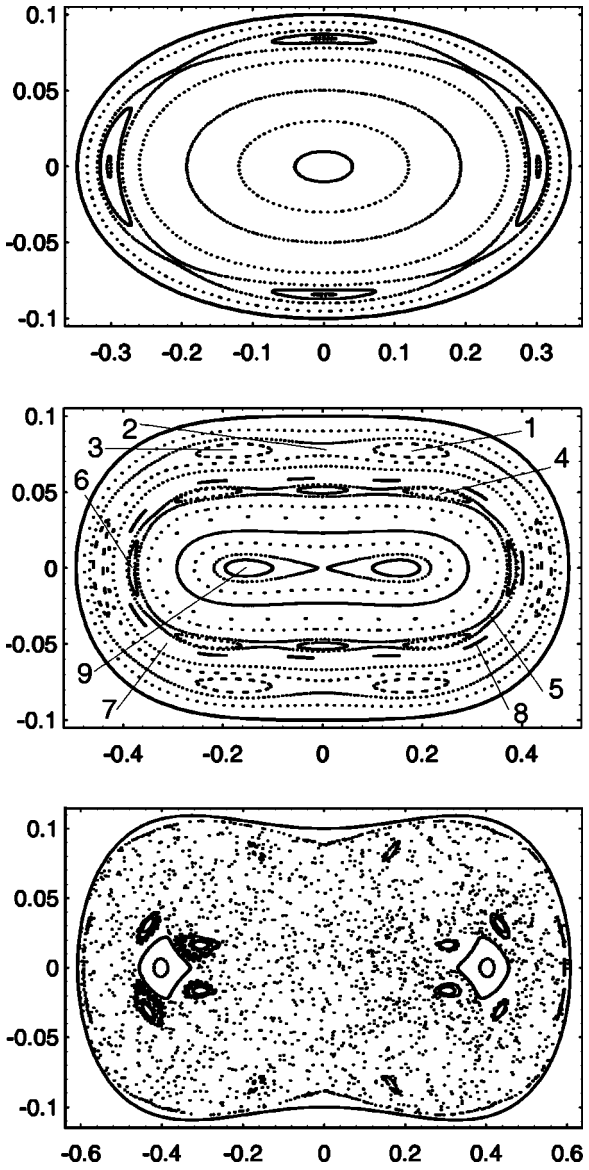

FIG. 4. Surfaces of section ξ-P_ξ ($P_z = 0$). From top to bottom $\delta = 0.6$, 0.7, and 0.757.

found for higher values of δ, where both circular and inclined trajectories disappear. More than this, for $\delta > 0.561$ more families are expected from bifurcations of axial and planar orbits. We rely again on surfaces of section in order to get a picture of the phase space. Thus, in Fig. 4 we present three surfaces of section. For $\delta = 0.6$ (top) we see elliptic and hyperbolic fixed points corresponding to stable and unstable bifurcations of the axial trajectory for $\delta = 0.5610$. For $\delta = 0.7$ (center) we identify several periodic trajectories: orbits (1, 2, 3) appear at $\delta = 0.6229$ as bifurcations of the z axis oscillation with triple period; orbits (4, 5, 6) bifurcate with fourfold period from the z axis oscillation at $\delta = 0.6500$; orbits (7, 8) are elevenfold bifurcations of the z axis oscillation that occurs at $\delta = 0.6429$.

For $\delta > 0.7$ the z axis oscillation becomes highly unstable and the phase space is gradually filled with chaos. The case $\delta = 0.757$ is presented at the bottom of Fig. 4, where chaos dominates the portrait alternating with chains of islands. The apparition of chaos seems to be related to the transition to instability of the z oscillations produced at $\delta = 0.6903$. Before this value all the solutions pass along the origin, but at this bifurcation, two almost vertical symmetric oscillations appear—orbit 9 in the center plot of Fig. 4 and its symmetric with respect to the z axis—that never pass through the origin.

IV. DISCUSSION

Despite all the orbits considered in the previous analysis being bounded orbits, not all of them have a physical meaning. In addition to being bounded orbits, they must be confined to the trap. Since the dimensions of the trap are given by the arrangement of the electrodes, and the orbits are bounded by the corresponding equipotential curve of constant energy, we can guarantee that, for a given δ, all the orbits will be real orbits if the equipotential curve remains confined between the electrodes. This fact is illustrated in Fig. 5. When δ is small, the equipotential curve spreads over a wide region of the z axis. Hence, most of the orbits around R_z will have a big size, and, therefore, unphysical meaning, while orbits around R_ξ will have a small size, being real trapped orbits. When δ tends to δ_ℓ, the equipotential curve is mainly localized along the ξ axis and, therefore, most orbits around R_ξ could be too large in size to be physical, while orbits around R_z will be real trapped orbits. A compensated behavior takes place for $0.3 \leqslant \delta \leqslant 0.5$ because the equipotential curve is well confined inside the trap—a situation usually achieved in real experiments [6].

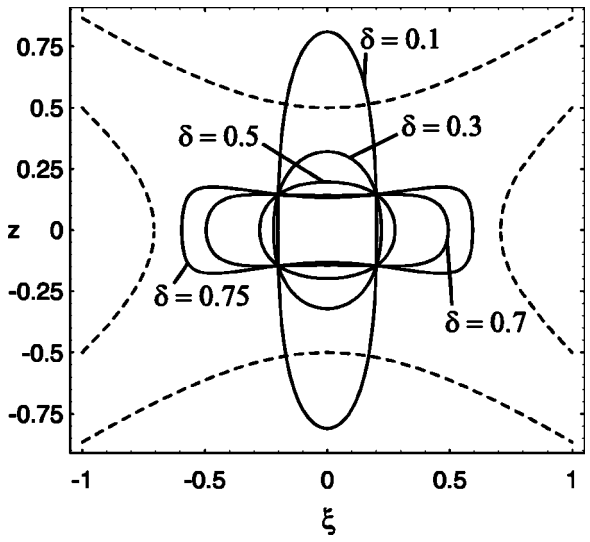

FIG. 5. Equipotential curves $W(\xi,z) = 1/200$ ($a = 0.2$). The dashed curves correspond to the electrodes.

On the other side, we can conclude that, for a wide range of values of δ, the phase space shows regular structure. The reason of this fact lies on that the effect of the octupolar perturbation can be mitigated by working with a cyclotron frequency w_c much bigger than the axial one w_z, i.e., $\delta \ll \delta_l$, corresponding to the usual experimental conditions: the so-called *hierarchy condition* arrives from the fact that slow magnetron motion is necessary in order to get an almost permanent ion confinement [8]. In this sense, for $\delta < 0.38$, the phase space structure is dominated by the only presence of the periodic orbits R_ξ and R_z. These periodic orbits are indicating that the behavior of the system is very near to its integrable limit (harmonic motion) for $a \to 0$. However, the general effect of increasing the control parameter δ is a pumping process through which periodic orbits emanate from vertical oscillations on the z axis and they continuously approach the (x,y) plane until ending as (horizontal) oscillations in that plane.

ACKNOWLEDGMENTS

M. Lara recognizes support from the Spanish Ministry of Technology and Science (Project No. ESP2002-02329). J. P. Salas recognizes support from the Spanish Ministry of Technology and Science (Project No. BFM2002-03157) and from the University of La Rioja (Project No. API02/20).

[1] S. C. Farantos, Int. Rev. Phys. Chem. **15**, 345 (1996); M. Davis, J. Chem. Phys. **107**, 1 (1997).
[2] S. Keshavamurthy and G. Ezra, J. Chem. Phys. **107**, 1 (1997).
[3] J.-M. Mao, K. A. Rapelje, S. J. Blodgett-Ford, and J. B. Delos, Phys. Rev. A **48**, 2117 (1993).
[4] F. M. Penning, Physica **3**, 873 (1936); H. Dehmelt, Rev. Mod. Phys. **62**, 525 (1990).
[5] D. J. Bate, Ph.D. thesis, Imperial College, London, 1991 (unpublished); D. J. Bate, K. Dholakia, R. C. Thompson, and D. C. Wilson, J. Mod. Opt. **39**, 2 (1992).
[6] G. Zs. K. Horvath, J. L. Hernandez-Pozos, K. Dholakia, J. Rink, D. M. Segal, and R. C. Thompson, Phys. Rev. A **57**, 1944 (1998).
[7] J. D. Jackson, *Classical Electrodynamics* (Wiley, New York, 1975).
[8] H. Dehmelt, Am. J. Phys. **58**, 1 (1990).